Macromolecules

ARTICLE

pubs.acs.org/Macromolecules

Synthesis of New Thermoplastic Elastomers by Silver Nanoparticles as Cross-Linker

Stefan Bokern, Ziyin Fan, Claudia Mattheis, Andreas Greiner, and Seema Agarwal*

Philipps-Universität Marburg, Hans-Meerwein-Strasse, 35032 Marburg, Germany

Supporting Information

ABSTRACT: A novel type of elastomers with silver nanoparticles (AgNP) as cross-linkers has been obtained by a quantitative one-phase bottom-up procedure based on α,ω-dimercapto-poly(*cis*-1,4-isoprene) (PIP). This telechelic polymer with high cis-content of >80% and near-quantitative functionalization degree has been synthesized in a one-pot procedure by anionic polymerization. It was cross-linked by coordination of the thiol groups to in-situ synthesized AgNP to yield a repeatedly melt-processable elastomer. It was found that the *E*-modulus increased up to an ideal ratio of AgNP to PIP and decreases drastically with AgNP oversaturation due to decreasing cross-linking density. Swelling experiments were in agreement with these results. The cross-linking of telechelic polymers with metal nanoparticles has been applied to other metals and polymers, leading to cross-linked materials in all cases. Antibacterial properties of the silver-containing elastomers were found by the Kirby−Bauer test.

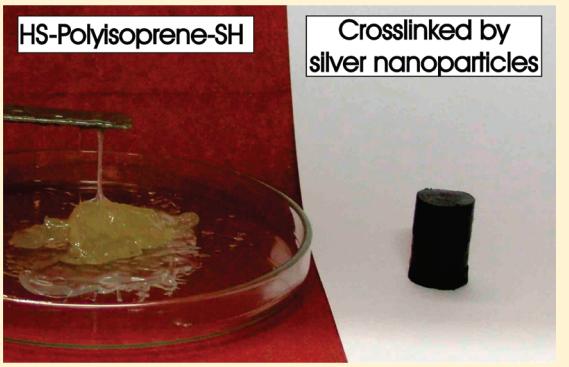

INTRODUCTION

Elastomers are generally polymers with low glass transition temperature, cross-linked either by chemical or by physical cross-linking.[1] Chemically cross-linked elastomers like vulcanized poly(*cis*-isoprene) have found widespread everyday applications despite being difficult to recycle due to the irreversible curing process.[2] Physical cross-linking generally is reversible, thus allowing simple processing by extrusion and recycling by melting. An important class of physically cross-linked, melt-processable elastomers are thermoplastic elastomers based on copolymers, for example poly(styrene−butadiene−styrene). Although a multitude of thermoplastic elastomers has been realized, the need for phase separation limits possible polymer combinations, making new cross-linking methods a desirable synthesis target.[3]

The synthesis of metal nanoparticle-cross-linked elastomers in particular appears to be a promising research topic because the interactions between metal nanoparticles like gold and silver and (thiolate-functionalized) stabilizers can reach the strength of chemical bonds, while still being reversible.[4]

Chemical groups which coordinate on metal nanoparticles may serve as cross-linking sites when these groups are linked to a polymer chain. Gold-cross-linked poly(vinyl alcohol) has been suggested for drug delivery applications,[5] and silver-cross-linked polymer microspheres have been applied for Raman spectroscopy.[6] FePt-nanoparticle-cross-linked siloxanes showed enhanced tensile strength.[7] It was also possible to cross-link telechelic polystyrene by CdSe nanoparticles.[8] Low molecular weight dithiols were used to bridge metal nanoparticles.[9]

We guessed that telechelic dithiols and AgNP should lead to polymer networks with AgNP as cross-linking sites. The resulting network should show macroscopic mechanical properties based directly on the polymer−nanoparticle interaction, with a large dependence on the molar nanoparticle:polymer ratio. For this study, we chose α,ω-dimercapto-polyisoprene (PIP) with high cis content as telechelic polymer, as the macroscopical transition from a polymer liquid to a polymer elastomer should be the result of successful nanoparticle cross-linking. The synthesis of PIP should be possible by anionic polymerization with a difunctional initiator.[10] Subsequent in-situ termination with ethylene sulfide should yield the desired PIP, similar to already known quantitative thiol-functionalization of polystyrene.[11] Finally, in-situ formation of AgNP should yield the polymer network with AgNP as cross-linker with elastomer properties depending on the ratio of AgNP to PIP (Figure 1). Although it is almost trivial to note for a silver-containing material, we also analyzed the antibacterial properties without going into too much detail here. However, this could become of further interest for a broader study, as natural polyisoprene from *Hevea brasilensis* is known to be biodegradable by bacteria like actinomycytes and other,[12] which could become at a later state an important issue for its application.

EXPERIMENTAL SECTION

Materials. Tetrahydrofuran (THF, BASF) and cyclohexane (BASF) were purified by distillation over sodium (Solvona) and stored under

Received: March 30, 2011
Revised: May 10, 2011
Published: June 02, 2011

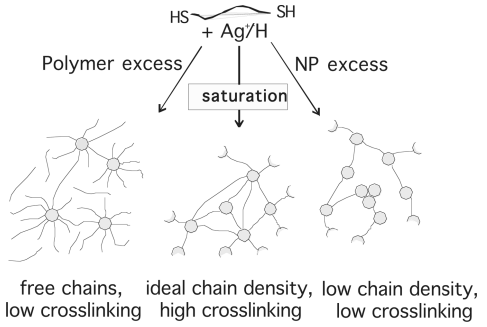

Figure 1. Hypothesis for AgNP-cross-linked PIP. An ideal saturation point should exist, where all nanoparticles have a maximal chain density and all polymer chains are bound. Either less or more nanoparticles lead to decreased cross-linking, either by free polymer chain ends or by aggregates and lowered chain density.

argon. All other solvents were distilled prior to use. Isoprene (Acros, 98%), triethylamine (Aldrich, 99.5%), *N,N,N′,N″,N‴*-pentamethyldiethylenetriamine (PMDETA, Aldrich, 99%), ethylene sulfide (Aldrich, 98%), and 1,3-diisopropenylbenzene (Aldrich, 97%) were distilled over calcium hydride and stored under argon. Silver trifluoroacetate (Merck) was recrystallized from diethyl ether. *tert*-Butyllithium (*t*-BuLi, Acros, 1.6 mol/L in pentane), Super-Hydride (lithium triethylborohydride solution, 1 mol/L in THF, Aldrich), palladium(II) acetate (Merck, for synthesis, 47% Pd), and tetrachloroauric acid trihydrate ($HAuCl_4$, ChemPur) were used as received. Mercapto-polystyrene was prepared by initiation of styrene polymerization in THF at −78 °C initiated by *s*-BuLi and terminated with 1 equiv of ethylene sulfide, as described elsewhere.[13] α,ω-Dimercapto-polystyrene was prepared by initiation of styrene polymerization in THF at 0 °C by naphthyl sodium and termination with 2 equiv of ethylene sulfide. PIP(3,4) was prepared by initiation of isoprene polymerization in THF at 0 °C by naphthyl sodium and termination with 2 equiv of ethylene sulfide.

Instrumentation. Gel permeation chromatography (GPC) was done by means of a Knauer system equipped with a PSS-SDV (10 μm) 50 × 8 mm^2 column and two columns 600 × 8 mm^2 at 25 °C, a differential refractive index detector, and a UV photometer using THF as eluent at a flow rate of 0.8 mL/min and linear polystyrene (PSS) as standard. ^1H (300.13 MHz) and ^{13}C (75.47 MHz) NMR spectra were recorded on Bruker Avance 300 A and Avance 300 B spectrometers, respectively, using $CDCl_3$ as solvent. Mettler thermal analyzers having 851 TG and 821 DSC moduluss were utilized for the thermal characterization of the polymers. Indium and zinc standards were used for temperature and enthalpy calibration of the 821 DSC modulus. Differential scanning calorimetric (DSC) scans were recorded in a nitrogen atmosphere (flow rate 80 mL/min) at a heating rate of 10 °C/min between −80 and +130 °C. The glass transition temperature (T_g) was taken as the inflection point of the observed shift in the baseline of the second heating cycle of a DSC scan. Thermal stability was determined by recording thermogravimetric (TG) traces in nitrogen atmosphere (flow rate 50 mL/min). A heating rate of 10 °C/min between 25 and 800 °C and a sample size of 8 ± 2 mg were used in each experiment. A Perkin-Elmer Lambda 9 UV/vis/NIR spectrophotometer was used for UV/vis absorption spectroscopy. The concentration of the samples was between 0.5 and 1.5 g/L, and the cuvette length was 0.5 cm. For XRD, a Philipps diffractometer with pixel detector has been used. Polymer films have been fixated on a silicon carrier, and a step length of 0.013° between 2θ = 10° and 50° has been used. The radiation source was Cu Kα radiation with a wavelength of 154 pm. Stress−strain measurements were done on a Zwick Roell BT-FR0.5TN.D14 equipped with a KAF-TC load sensor. The samples (50 × 10 × 1 mm) were prepared by heat pressing at 20 bar pressure and 100 °C for 3 min, followed by cooling to 21 °C over 2 min.

Scheme 1. One-Pot Synthesis of PIP

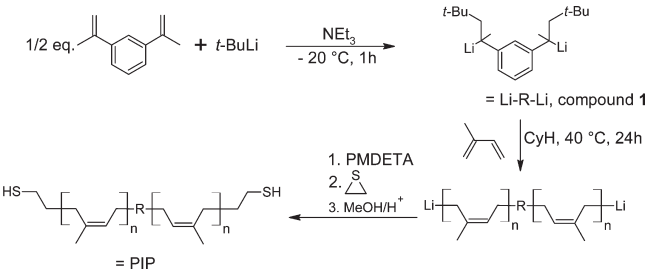

Measurements have been done at 21 °C after keeping the samples for at least 20 min at this temperature. The measurement speed was 50 mm/min, and the plate-to-plate distance was 20 mm.

Synthesis of the Difunctional Lithium Initiator (Compound 1). In a flame-dried Schlenk flask, *t*-BuLi in pentane (18.75 mL, 30 mmol, 2 equiv) was cooled to −20 °C. Triethylamine (4.16 mL, 30 mmol, 2 equiv) was added. Diisopropenylbenzene (2.57 mL, 15 mmol, 1 equiv) was added dropwise over 20 min; immediately a deep-red color developed. The initiator was used immediately after 2 h of stirring. Concentration (calcd): 0.6 mol/L.

Synthesis of α,ω-Dimercapto-poly(*cis*-1,4-isoprene) (PIP). The synthesis of sample PIP_{4100} is described. In a flame-dried 1 L Schlenk flask, isoprene (74 mL, 0.74 mol, 43 equiv) was dissolved in dry cyclohexane (250 mL) under argon and cooled to 0 °C. The initiator solution (17 mmol, 30 mL, 1 equiv) was added dropwise to quench eventual trace amounts of water and oxygen. After addition of the initiator, the now slightly yellow solution was heated to 40 °C for 18 h for polymerization, resulting in a very viscous solution. To remove eventual monomer residue, the solution was concentrated to a volume of 400 mL at 0 °C in oil pump vacuum, resulting in near-complete gelation. PMDETA (7.1 mL, 34 mmol, 2 equiv) was added, the viscosity decreased drastically, and the color changed from yellow to a dark orange. After 10 min, ethylene sulfide (2.0 mL, 34 mmol, 2.1 equiv) was added dropwise, resulting in a color change from deep orange to a pale yellow and an increase in viscosity. After 20 min, the reaction was quenched with methanol (10 mL), and a near-complete loss of viscosity and color was observed. The solution was filtered through a column to remove salts, and the solvent was removed at room temperature in vacuum. For work-up, the viscous yellow polymer was redissolved in 400 mL of cyclohexane and precipitated in 4 L of methanol as a very viscous oil. After decantation, the residue was washed with methanol and dried in vacuum at room temperature for 18 h. The product was isolated as clear yellow oil and was protected against air and light until further reactions. Yield: 54.6 g (96%). M_{theor} = 3323, M_{NMR} = 4106. UV/vis: λ_{max} = 223 nm. TGA: T_{decay} = 365 °C, T_g = −59 °C. Degree of functionalization: >95% (NMR). For other molecular weights, the amount of isoprene and solvent was changed accordingly.

Synthesis of Silver Nanoparticle-Cross-Linked PIP. The synthesis is described for the sample $PIP_{9210}Ag_{5.7}$. Silver trifluoroacetate (0.68 g, 3.1 mmol, 5.7 equiv) was dissolved in 20 mL of THF, and a slight excess of trifluoroacetic acid (0.24 mL, 3.1 mmol, 2 equiv) was added to quench silver−thiolate coordination. PIP in THF (5 g, 0.54 mmol, 1 equiv in 20 mL of THF) was added, and the solution was kept at 20 °C. After 5 min, a large excess of triethylboron hydride in THF (20 mL, 20 mmol, 37 equiv) was added dropwise under vigorous stirring; immediately upon addition a deep-brown gel formed. After 20 min, the reaction was quenched with 4 mL of methanol. The product was precipitated in 400 mL of methanol/HCl (100:1) as solid brown rubberlike flakes, filtered off, washed, and dried at 60 °C in vacuum overnight. Yield: quantitative. For all other samples, the amount of silver trifluoroacetate

dx.doi.org/10.1021/ma200738b |*Macromolecules* 2011, 44, 5036–5042

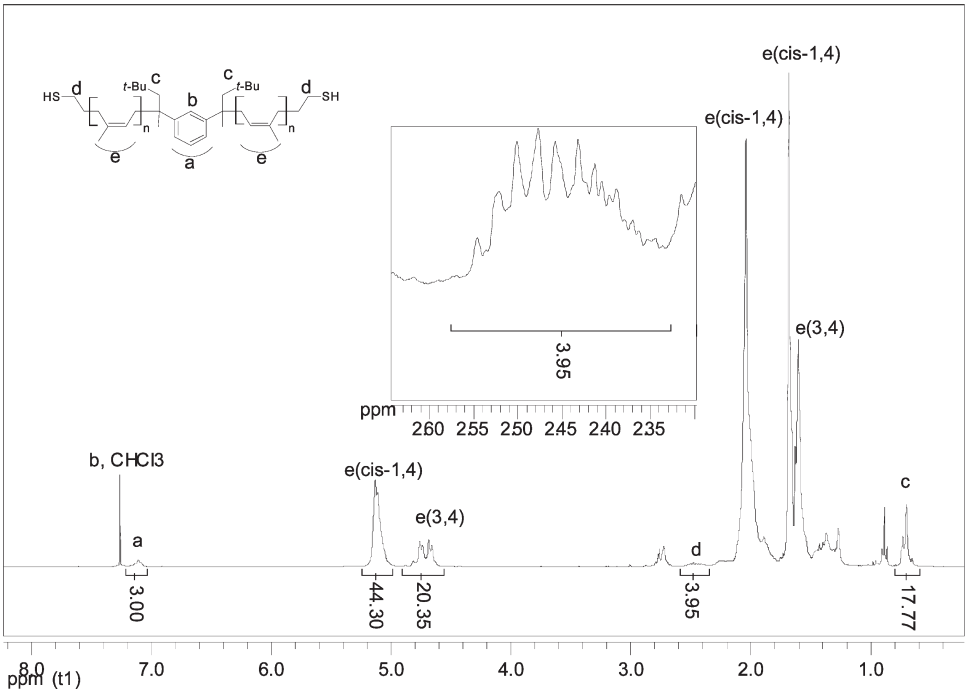

Figure 2. ^{1}H NMR of PIP, sample PIP_{4100}. Characteristic signals are marked. The signals between δ = 4.6 and 5.2 ppm have been used to calculate the cis content of the polymer. The multiplet at δ = 2.45 ppm is characteristic for the CH_2−SH end group.

was changed and all other parameters including the amount of reduction agent were kept identical. For very soft materials, the product was not filtered off but simply removed by decantation and washed. The comparison samples of silver-free PIP were treated the same way.

RESULTS AND DISCUSSION

PIP has been synthesized here by anionic polymerization using dilithiated compound **1** as initiator in unpolar solvent, which has been obtained by nucleophilic addition of *t*-BuLi to diisopropenylbenzene (Scheme 1).[10] This route is similar to a described synthesis of α,ω-dimercapto-poly(*cis*-butadiene). However, the degree of functionalization has not been determined, and we assume it to be low due to gelation problems we describe here for poly(*cis*-isoprene).[14]

After polymerization, the cyclohexane solution of PIP showed a high viscosity up to complete gelation even at low polymer content. This resulted from end-group cross-linking by Li−C aggregates, most probably tetramers or hexamers which are known to form with aliphatic lithium compounds under these conditions.[15] The viscosity could be reduced significantly by addition of 5−10 equiv of THF, which leads to Li−C dimer formation.[16] The addition of ethylene sulfide led to immediate and complete gelation of the whole mixture and incomplete end-functionalization at about 50%. The problem of gelation by aggregate formation has been avoided completely by addition of PMDETA after isoprene polymerization, which is a far stronger coordinating agent than THF and is known to yield monomeric forms of organolithium compounds in unpolar solvents.[17] Here, the solution viscosity decreased drastically upon addition of PMDETA, and no gelation occurred after ethylene sulfide addition. Addition of PMDETA also had the advantage of increasing the reactivity of the chain end drastically, allowing functionalization with exactly one unit of ethylene sulfide by simple observation of color change (from bright orange to pale yellow).

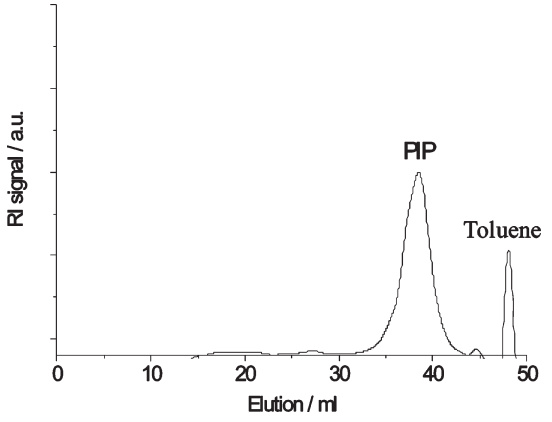

Figure 3. THF-GPC of PIP (sample PIP_{4100}) showed a monomodal signal, ensuring well-controlled reaction conditions.

In NMR, the methylene groups next to the thiols were found at δ = 2.45 ppm, nearly identical to literature examples of aliphatic $-CH_2-SH$ groups (Figure 2).[18] The signal was not found in the NMR of the unfunctionalized polymer, synthesized by quenching with methanol. It has been found that the functionalization degree is close to be quantitative.

The yield of polymerization was quantitative, and the theoretical molecular weight was slightly higher than the experimental molecular weight. PIP was completely soluble in unpolar solvents and showed a monomodal distribution in GPC, indicating a complete absence of theoretically possible cross-linking reactions by addition of the thiols to double bonds or disulfide formation (Figure 3). Exposure to sunlight had to be avoided in order to avoid unwanted thiol−ene cross-linking reactions.

dx.doi.org/10.1021/ma200738b |*Macromolecules* 2011, 44, 5036–5042

Table 1. AgNP-Cross-Linked PIP as a Function of the Ratio of Ag:PIP and Molecular Weight of PIP[a]

sample	Ag:PIP	$m_{residue}$/wt %	T_g/°C	E_{mod}/MPa
PIP_{4100}	0	1	−59	−[b]
$PIP_{4100}Ag_{0.5}$	0.5	3	−53	−[c]
$PIP_{4100}Ag_{1.2}$	1.2	6	−52	−[c]
$PIP_{4100}Ag_{2.3}$	2.3	9	−51	0.64
$PIP_{4100}Ag_{4.7}$	4.7	10	−54	1.12
$PIP_{4100}Ag_{9.3}$	9.3	23	−51	0.35
$PIP_{4100}Ag_{14}$	14.0	26	−53	0.20
PIP_{9210}	0	1	−62	−[b]
$PIP_{9210}Ag_{0.7}$	0.7	3	−58	−[c]
$PIP_{9210}Ag_{1.4}$	1.4	5	−59	0.22
$PIP_{9210}Ag_{2.9}$	2.9	8	−59	0.44
$PIP_{9210}Ag_{5.7}$	5.7	12	−58	0.52
$PIP_{9210}Ag_{11.4}$	11.4	16	−58	−[c]
$PIP_{9210}Ag_{17}$	17.0	17	−58	−[c]

[a] Ag:PIP describes the molar ratio of silver salt to polymer during nanoparticle synthesis, and $m_{residue}$ describes the residue in TGA at 750 °C. [b] Not measurable; sample was a very viscous oil. [c] Not measurable; sample was a tar-like sticky solid and not form-stable at room temperature.

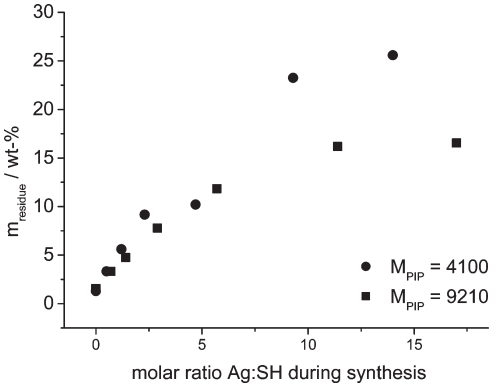

Figure 4. Ash yield of TGA measurements of AgNP-PIP as a function of Ag:SH ratio.

Following the previously published concept,[13] AgNPs were obtained by addition of silver trifluoroacetate to PIP, followed by Super-Hydride reduction. Different ratios of silver trifluoroacetate:PIP as well as different molecular weights of PIP resulted in composites with different AgNP content, different glass transition temperatures, and different *E*-moduli (Table 1).

It was found by TGA that ash yield, which represents the silver residue, rose with the used amount of silver salt (Figure 4), close to the theoretically expected amount of silver (e.g., sample $PIP_{4100}Ag_{14}$: $M_{Ag,theor}$ = 16.7 wt %, $M_{Ag,found}$ = 16.5 wt %). The main degradation in TGA experiments is most likely due to the degradation of the PIP main chain. TGA measurements showed no significant change in the main degradation temperature depending on the nanoparticle content. In all cases the main thermal degradation occurred around 360 °C.

The presence of AgNP was proven by TEM analysis and XRD. AgNP with diameters of about 2 nm were found in TEM (Figure 5). The formation of a low number of larger aggregates could not be avoided due to the gelation of the reaction mixture due to the cross-linking process.

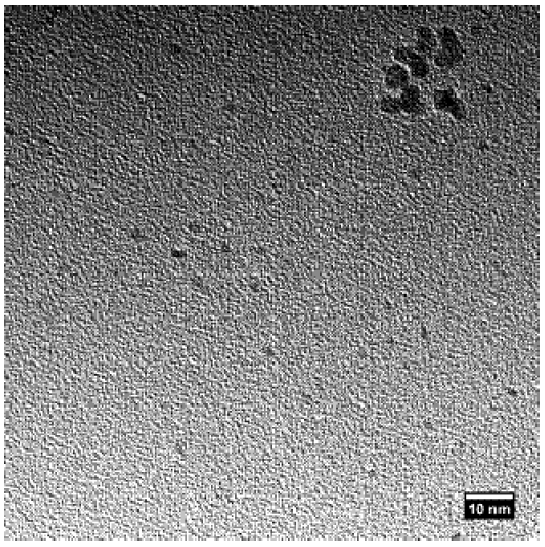

Figure 5. TEM of the sample $PIP_{9210}Ag_{0.7}$. Most particles are low-size silver nanoparticles with uniform diameters of around 2 nm, but agglomerates are also observed.

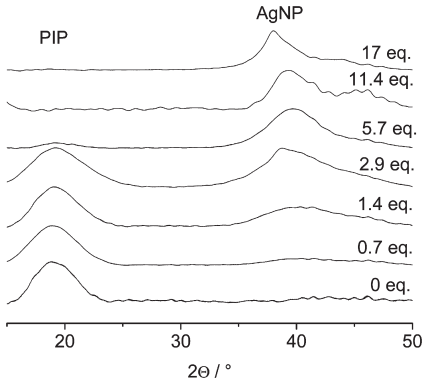

Figure 6. XRD measurements of AgNP-cross-linked PIP (M = 9210). The relative amorphous polyisoprene halo intensity decreases with the AgNP content.

In XRD, a broadened signal at 2ϕ = 38°−42° was found, characteristic for AgNP (Figure 6). The ratio of the amorphous polyisoprene halo at 2ϕ = 17°−22° to the AgNP signal decreased drastically with the amount of silver, in agreement with the increase of AgNP content found by TGA.

During synthesis, it was observed that the viscosity of the reaction mixture increased drastically upon addition of Super-Hydride. In some cases, even complete gelation occurred at low polymer contents of around 10 wt %. This effect did not occur without the silver salt. This indicates a successful cross-linking of the polymer end groups by coordination to silver nanoparticles, which should have a significant effect on the mechanical properties. Indeed, after work-up, a solid brown to black substance was isolated in quantitative yield, with tar-like to rubber-like composition, depending on silver content. Surprisingly, this rubber-like material in best case becomes liquid upon heating above 90 °C and rubbery again upon cooling to room temperature. Once cooled to room temperature, this material displayed shape stability with unchanged elastomer properties over a period of at least 4 months and can be reprocessed at any time in a

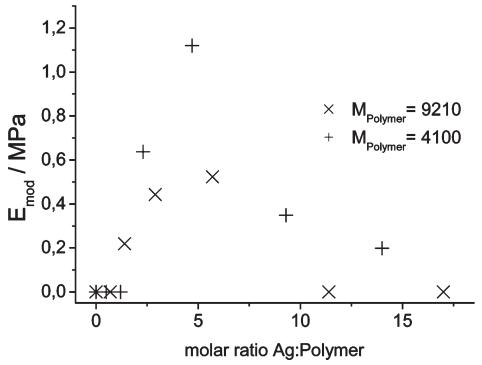

Figure 7. *E*-modulus of AgNP-cross-linked PIP as a function of the Ag:PIP. If the sample was not form stable and too soft for processing, an *E*-modulus of 0 MPa has been assumed.

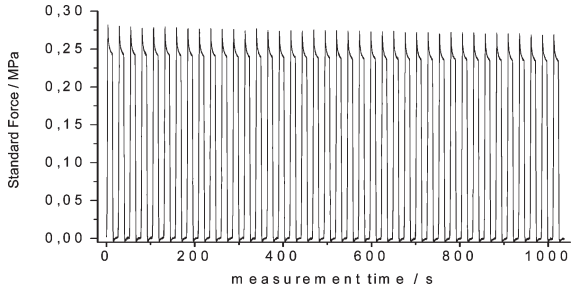

Figure 8. Stress−strain measurement of sample $PIP_{9210}Ag_{5.7}$, cyclic elongation to 15% strain (50 cycles, 10 s strain, 10 s relaxation). The strain was completely reversible, and creep was not observed.

thermoplastic fashion. Thereby, it can be coined as a novel thermoplastic material. The thermoplastic behavior of the AgNP-cross-linked PIP is most likely due to the noncovalent nature of the sulfur−silver coordination. It has been heat pressed into sheet form and showed elastic behavior which was strongly dependent on the ratio of AgNP:PIP. It was observed that the *E*-modulus rose up to a certain point independently from the molecular weight of PIP (Figure 7). The elongation at break was antiproportional to the measured *E*-moduli. The samples with the highest *E*-modulus broke at an elongation of 22% ($PIP_{4100}Ag_{4.7}$) and 51% ($PIP_{9210}Ag_{5.7}$).

The *E*-modulus is known to be directly proportional to the cross-linking density.[19] These results are in accordance with the hypothesis regarding an ideal saturation point where all polymer chain ends are coordinated to nanoparticles and all nanoparticles have a maximal chain density (compare Figure 1). The cross-linking density naturally is lower for the polymer with higher polymer weight due to longer soft segments, explaining the difference between both characterized polymers. The measured properties do not change after recycling the material by heat pressing. Application of cyclic stress−strain measurement showed completely reversible strain and proved that indeed a form-stable elastomer was synthesized (Figure 8).

If an ideal system of AgNP with uniform diameter of 2.0 nm is assumed, each AgNP contains about 520 atoms (assuming a density of 10.45 g/cm), leading to a theoretical molecular weight of the AuNP of 56 100 g/mol. For a well-cross-linked sample with an AgNP content of 12 wt % (sample $PS_{9210}Ag_{5.7}$, every PIP chain with M_n = 9210 g/mol carries two thiol groups), this leads to 89 thiol groups for every AgNP. This is a surprisingly good

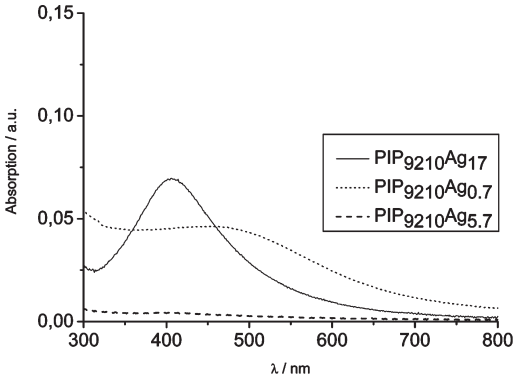

Figure 9. UV/vis of the hexane extract after 24 h for different silver contents, normalized to polyisoprene absorption.

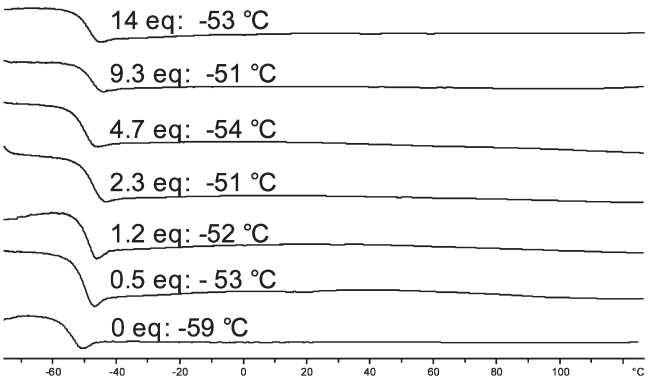

Figure 10. DSC thermograms of different samples of AgNP-cross-linked PIP (sample PIP_{4100}).

match with a model for dodecanethiol-stabilized gold nanoparticles, where 91 thiol groups for every AuNP (2.0 nm diameter) are calculated to be the maximal density.

Although some rough estimates and assumption were made, these strengthen the hypothesis of a nanoparticle saturation point.[20]

In order to gain a better understanding of the nature of this new thermoplastic elastomer, further analysis was undertaken by swelling experiments and DSC analysis. The formation of a network of AgNP and PIP was verified by swelling experiments, where after 24 h in hexane a reversible swelling of 570 wt % ($PIP_{9210}Ag_{5.7}$) and no nanoparticle dispersion were observed. In samples with either less or more AgNP, the supernatant contained AgNP due to the lower cross-linking density. This has been verified by UV/vis measurements.

UV/vis spectra of the hexane extract after 24 h of extraction of PIP cross-linked by different amount of AgNP are shown in Figure 9. In the samples $PIP_{9210}Ag_{0.7}$ and $PIP_{9210}Ag_{17}$, large amounts of dispersed AgNPs are detected in the extract by their characteristic plasmon absorption. The plasmon absorption in both cases is within the expected range for silver nanoparticles; their shift is explained by different aggregation states.[21] The presence of AgNP shows that both samples are most likely not fully cross-linked and can dispersed partially upon treatment with hexane. In contrast, $PIP_{9210}Ag_{5.7}$ did not show any signals for redispersed silver-containing material due to heavy cross-linking.

The glass transition temperature showed a low dependency on the AgNP content, rising from −60 °C for the pure PIP to

Table 2. Analyzed Systems Similar to the Silver-Cross-Linked PIP and Cross-Linking Behavior Determined by Swelling Experiments[a]

polymer	metal	after solvent addition
PS-SH	Ag, Au, Pd	dispersions (THF, $CHCl_3$, CH_2Cl_2, toluene)
HS-PS-SH	Ag, Au	swollen gels (THF)
PIP(3,4)-SH[b]	Ag, Au	dispersions (THF, hexane)
HS-PIP(3,4)-SH[c]	Ag, Au	swollen gels (THF, hexane)
PIP	Au, Pd, Co	swollen gels (hexane)

[a] All cross-linked telechelic polymers show to form gels in solvent, while the monofunctional polymers form nanoparticle dispersions. [b] ω-Thiol-poly(3,4-isoprene). [c] α,ω-Dithiol-poly(3,4-isoprene).

−54 °C for the nanoparticle-containing samples (Figure 10). A similar increase in glass transition temperature has been observed previously for ω-thiol-polystyrene/AgNP.[13] This minor increase is also in accordance with conventional cross-linking of polymers[22] and shows that the structure of the polymer itself was not changed by the reaction procedure. It is known that thiol-stabilized metal nanoparticles can undergo a melt-like phase transition (hexadecanethiol-stabilized gold nanoparticles: T_m = 50−60 °C); reversible desorption of the thiol group may also be an explanation. The melt-like phase transition is known to result in a weak and very broad signal in DSC, which can be expected to be even weaker and broader when using polymers as stabilizers.[23] We assume this to be the reason why the synthesized AgNP cross-linked PIP melts but does not show additional DSC signals.

To ensure that the observed cross-linking was not a phenomenon encountered with polyisoprene and silver only, some similar polymer/metal combinations have been prepared, and the cross-linking has been determined by observation of the material after solvent addition (Table 2). It has been found that, when using a monofunctional polymer, no three-dimensional cross-linking was observed. All materials were redispersible easily and passed a 200 nm syringe filter completely. When a difunctional polymer was used, none of the samples were redispersible. In all cases, a swelling and formation of suspended gel particles were observed, which were not able to pass a 200 nm filter. It was observed that mechanical properties differed greatly with the same polymer depending on the metal, indicating a direct relation between coordination strength and mechanical properties, which may be quantified in a future publication.

Because of the presence of AgNP's in the AgNP cross-linked PIP, we assumed a strong antibacterial activity of the resulting rubber. This was proven by the Kirby−Bauer test, which showed that *Escherichia coli* did not grow at all on AgNP-cross-linked PIP. In contrast, pure PIP showed strong bacteria growth on the material. AgNP-cross-linked PIP did not show any leaching of silver, which would have been indicated by an inhibition zone in the Kirby−Bauer tests (Supporting Information).

CONCLUSIONS

Silver nanoparticles were used successfully as cross-linker for telechelic polyisoprene, thereby forming a rubbery material with elastomer and antibacterial properties. Surprisingly, these new elastomers are melt-processable at elevated temperatures. The elastomer properties are scaling directly with the ratio of AgNP and thiol end-group content. While the bulk application of AgNP as simple elastomer cross-linker may be too expensive for industrial application, we are convinced that this new concept for thermoplastic elastomers will be of interest due to the high functionality of silver nanoparticles and will be extended significantly in future by change of the nature, size, and shape of the metal nanoparticles and by exploitation of the biological, optical, electrical, and magnetic properties of metal nanoparticles. On top of this, the new concept can be applied to other type of nanoparticles as well, such as metal oxide nanoparticles, giving a wealth of new opportunities for a new class of thermoplastic elastomers different from those known until now as classical thermoplastic elastomers.

ASSOCIATED CONTENT

Supporting Information. Swelling experiments, stress−strain measurement, and tests of antibacterial activity. This material is available free of charge via the Internet at http://pubs.acs.org.

AUTHOR INFORMATION

Corresponding Author

*Tel ++49-6421-2825755, Fax ++49-6421-2825785, e-mail agarwal@staff.uni-marburg.de.

REFERENCES

(1) Abts, G. *Einführung in die Kautschuktechnologie*; Hanser: Munich, 2007.
(2) Adhikari, B.; De, D.; Maiti, S. *Prog. Polym. Sci.* **2000**, *25* (7), 909–948.
(3) Holden, G. *Thermoplastic Elastomers*; John Wiley & Sons, Inc.: New York, 2002.
(4) Konopka, M.; Rousseau, R.; Stich, I.; Marx, D. *J. Am. Chem. Soc.* **2004**, *126*, 12103–12111.
(5) Moreno, M.; Hernández, R.; López, D. *Eur. Polym. J.* **2010**, *46* (11), 2099–2104.
(6) Farah, A. A.; Alvarez-Puebla, R. A.; Fenniri, H. *J. Colloid Interface Sci.* **2008**, *319* (2), 572–576.
(7) Song, H. M.; Kim, Y. J.; Park, J. H. *J. Phys. Chem. C* **2008**, *112* (14), 5397–5404.
(8) Kim, J.; Kim, S. S.; Kim, K. H.; Jin, Y. H.; Hong, S. M.; Hwang, S. S.; Cho, B.-G.; Shin, D. Y.; Im, S. S. *Polymer* **2004**, *45* (10), 3527–3533.
(9) Brust, M.; Schiffrin, D. J.; Bethell, D.; Kiely, C. *J. Adv. Mater.* **1995**, *7* (9), 795–797.
(10) Yu, Y. S.; Dubois, P.; Jerome, R.; Teyssie, P. *Macromolecules* **1996**, *29* (8), 2738–2745.
(11) Quirk, R. P.; Ocampo, M.; Polce, M. J.; Wesdemiotis, C. *Macromolecules* **2007**, *40* (7), 2352–2360.
(12) Linos, A.; Berekaa, M. M.; Reichelt, R.; Keller, U.; Schmitt, J.; Flemming, H.-C.; Kroppenstedt, R. M.; Steinbuchel, A. *Appl. Environ. Microbiol.* **2000**, *66* (4), 1639–1645and references therein.
(13) Bokern, S.; Getze, J.; Agarwal, S.; Greiner, A. *Polymer* **2011**, *52* (4), 912–920.
(14) Tung, L. H.; Lo, G. Y. S.; Griggs, J. A. *J. Polym. Sci., Polym. Chem. Ed.* **1985**, *23* (5), 1551–1568.
(15) Elschenbroich, C. *Organometallchemie*; Teubner B.G. GmbH: Berlin, 2008.
(16) Gessner, V. H.; Däschlein, C.; Strohmann, C. *Chem.—Eur. J.* **2009**, *15* (14), 3320–3334.
(17) Strohmann, C.; Gessner, V. H. *Angew. Chem., Int. Ed.* **2007**, *46* (24), 4566–4569.
(18) Spectral Database for Organic Compounds (SDBS); 1H-NMR 1-propanethiol; SDBS No. 5147HSP-03-679; http://riodb01.ibase.aist.go.jp/sdbs/ (accessed February 7, 2011).

(19) Liu, Y.; Huglin, M. B. *Polymer* **1995**, *36* (8), 1715–1718.
(20) Hostetler, M. J.; Wingate, J. E.; Zhong, C.-J.; Harris, J. E.; Vachet, R. W.; Clark, M. R.; Londono, J. D.; Green, S. J.; Stokes, J. J.; Wignall, G. D.; Glish, G. L.; Porter, M. D.; Evans, N. D.; Murray, R. W. *Langmuir* **1998**, *14* (1), 17–30.
(21) Zhang, J.; Malicka, J.; Gryczynski, I.; Lakowicz, J. R. *Anal. Biochem.* **2004**, *330* (1), 81–86.
(22) Wang, Z.; Zhang, X.; Zhang, Y.; Zhang, Y.; Zhou, W. *J. Appl. Polym. Sci.* **2003**, *87* (13), 2057–2062.
(23) Sidhaye, D. S.; Prasad, B. L. V. *Chem. Mater.* **2010**, *22* (5), 1680–1685.